

Design of an Automated, High-Throughput Optical
Characterization Tool for Photovoltaics

by

Anthony Troupe

Submitted to the Department of Mechanical Engineering
in Partial Fulfillment of the Requirements for the Degree of

Bachelor of Science in Mechanical Engineering

at the

Massachusetts Institute of Technology

June 2021

© 2021 Anthony Troupe. All rights reserved.

The author hereby grants to MIT permission to reproduce and to distribute
publicly paper and electronic copies of this thesis document in whole or in
part in any medium now known or hereafter created.

Signature of Author: _____
Department of Mechanical Engineering
May 14, 2021

Certified by: _____
Vladimir Bulović
Professor of Electrical Engineering
Thesis Supervisor

Accepted by: _____
Kenneth Kamrin
Associate Professor of Mechanical Engineering
Undergraduate Officer

Design of an Automated, High-Throughput Optical Characterization Tool for Photovoltaics

by

Anthony Troupe

Submitted to the Department of Mechanical Engineering
on May 14, 2021 in Partial Fulfillment of the
Requirements for the Degree of

Bachelor of Science in Mechanical Engineering

Abstract

Photovoltaic (PV) devices are traditionally optimized through an iterative, top-down engineering approach in which many devices are built, tested, and studied to determine where performance improvements can be made. Researchers typically perform multiple measurements on each device using various manual characterization tools. This practice is ultimately time-intensive, inefficient, and expensive. This thesis documents the development of an automated, large-format characterization tool capable of performing multiple optical measurements simultaneously in order to address existing PV characterization inefficiencies. The resulting prototype demonstrates potential to serve as a high-throughput research tool that could ultimately advance the pace of future PV research.

Thesis Supervisor: Vladimir Bulović
Title: Professor of Electrical Engineering

Acknowledgements

I would like to thank my thesis advisor, Vladimir Bulović, along with the rest of the TATA-MIT GridEdge Solar Research Program for their support with this project. I would also like to specifically thank Dane deQuilettes and Brandon Motes for giving me the opportunity to join their team. Dane and Brandon initiated efforts towards this project prior to my involvement and developed many solutions that later served as a basis for my contributions. As the GridEdge Solar team lead, Dane has been an excellent mentor and helped drive the vision of this project from its beginnings. Working alongside Brandon has also been incredibly rewarding and much of this project's success can be attributed to his involvement in all aspects of the tools development.

Table of Contents

Abstract	2
Acknowledgements	3
Table of Contents	4
List of Figures	5
List of Tables	6
1. Introduction	7
2. Background	8
2.1 TATA-MIT GridEdge Solar Research Program	8
2.2 Perovskite Characterization	9
2.3 Previous Work	10
3. Solution Approach	11
3.1 Design Goals	11
3.2 Operating Principles	12
4. Optical Probe Head Assembly	15
4.1 Purpose & Requirements	15
4.2 Probe Head	16
4.3 Kinematic Mount Coupling	21
5. Motion Platform	22
5.1 Purpose & Requirements	22
5.2 Tool Architecture	23
5.3 Motion Components	27
5.4 Fabrication & Assembly	29
6. Design Evaluation	30
6.1 Sample Data Collection	30
6.2 Shortcomings and Future Work	31
7. Conclusions	33
8. References	34

List of Figures

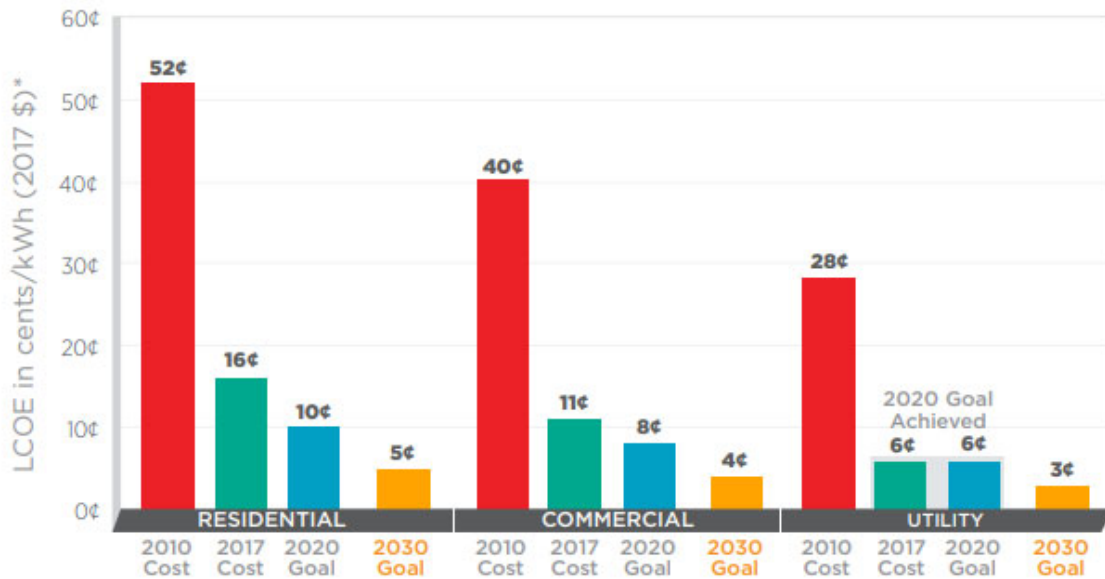
Figure 1-1:	SETO SunShot 2030 PV LCOE targets [1]	7
Figure 2-1:	Example of PL and TRPL data [5]	9
Figure 2-2:	Previous optical characterization tool prototype from January 2020	10
Figure 3-1:	Tool subcomponents and process flow	13
Figure 4-1:	Probe head rendering	16
Figure 4-2:	Illustrated example of optical data collection	17
Figure 4-3:	Properties of a Lambertian emitter	18
Figure 4-4:	Optics mounting interface of the probe head	19
Figure 4-5:	FEA of the probe head to determine local deflection at the optics	19
Figure 4-6:	Exploded view of the optical probe head assembly	20
Figure 4-7:	Closer view of the kinematic mount coupling	21
Figure 5-1:	Tool rendering with motion coordinate axes	23
Figure 5-2:	Characterization tool working volume	24
Figure 5-3:	Base plate working drawings and weight-reduction pockets	25
Figure 5-4:	FEA of y-axis gantry cross member to determine maximum deflection	26
Figure 5-5:	Y-axis gantry cross member cross-section	27
Figure 5-6:	Stepper motor torque-speed curve [8]	29
Figure 5-7:	Images of the assembled optical characterization tool prototype	30
Figure 6-1:	Sample PL and TRPL data collected with the tool prototype	31

List of Tables

TABLE 3-1: Overall design goals	11
TABLE 4-1: Optical probe head assembly design requirements	15
TABLE 5-1: Motion platform design requirements	22

1. Introduction

Photovoltaics (PVs) present a compelling opportunity to sustainably generate electricity and mitigate the impending threats of climate change. As such, the continued advancement of PV technologies is critical to the future of sustainable energy generation. The necessity for rapid improvements in PV performance is readily exemplified by levelized cost of energy (LCOE) targets published by the United States Solar Energy Technologies Office (SETO), shown in Figure 1-1.



*Levelized cost of electricity (LCOE) progress and targets are calculated based on average U.S. climate and without the ITC or state/local incentives. The residential and commercial goals have been adjusted for inflation from 2010-17.

Figure 1-1: LCOE targets from the SETO SunShot 2030 Goals Report. 2030 goals include LCOE of \$0.03/kWh for utility-scale PV. This figure is adapted from its source [1].

For residential, commercial, and utility scale PV, SETO is targeting over 50% reductions in LCOE from 2020 to 2030. At these costs, electricity from utility-scale PV would be among the least expensive options for establishing new power generation capacity in locations across the United States. In many areas of the country with greater insolation, purchasing and building new PV infrastructure would also be competitive with the variable cost associated with continuing to operate existing nonrenewable electricity generators [1]. The potential economic advantages of PVs could therefore lead to significant increases in demand for PV generation capacity, expanding well beyond the current 2.2% of US generation capacity currently attributed to utility-scale PV (as of 2020) [2].

Despite the demand for accelerated PV research, the current process of developing novel PV devices is inefficient and time-intensive. Typically, devices are built, tested, and then studied to determine where incremental improvements in performance can be made. This process is continuously repeated, with the goal of building upon insights discovered from batch after batch of solar cells. The pace of development through this iterative approach is largely related to the rate in which devices can be created and then meaningfully analyzed. Existing research infrastructure is not optimally configured to address this method of research and development. For example, the process of characterizing devices oftentimes requires manual operation of numerous types of measurement equipment and further organization of various data outputs in order to offer meaningful understanding of a given devices performance.

The development of a PV characterization tool that can address the shortcomings of traditional research equipment offers the potential to enable accelerated improvements in PV technologies. This project attempts to remediate the inefficiencies of existing data collection methods through the development of an automated, large-format characterization tool capable of performing multiple optical measurements simultaneously. More specifically, this thesis focuses on the mechanical design and development of an optical probe head and its corresponding motion platform within the tool.

2. Background

2.1 TATA-MIT GridEdge Solar Research Program

The efforts described within this thesis were completed as part of the TATA-MIT GridEdge Solar Research Program. GridEdge Solar is an interdisciplinary research program working toward scalable design and manufacturing of lightweight, flexible solar cells. The team is specifically focused on emerging PV architectures such as perovskites.

Perovskites are a family of materials with a specific crystalline structure that can potentially offer several advantages over more mature PV architectures [3]. Most notably, perovskites are comprised of earth-abundant materials and are typically fabricated in thin-film configurations. These qualities present opportunities to save costs and produce high volumes of solar cells through roll-to-roll manufacturing processes. Perovskites are also lightweight and flexible, opening several unique market opportunities that leverage these qualities.

2.2 Perovskite Characterization

A multitude of material properties are of interest to researchers when evaluating the performance of a particular PV device. The analysis methods and characterization techniques researchers choose to pursue is directly related to the PV architecture being studied. As noted, GridEdge Solar is predominately interested in the emerging field of perovskites. Therefore, this project focused on characterization techniques most relevant to the study of perovskite semiconductors.

Two types of measurement – photoluminescence (PL) and time-resolved photoluminescence (TRPL) – were of particular interest when developing the improved characterization tool. Photoluminescence is a measure of the light emissions from a photoactive material following optical excitation. In PV applications, PL measurements can be applied to inform researchers on a wide variety of characteristics that impact a solar cells performance, including quantum efficiency, recombination mechanisms, and transport phenomena [4]. TRPL measures the photoexcited charge carrier lifetime, where longer lived carriers have a higher probability of reaching electrodes, resulting in increased efficiency. Examples of data a researcher may generate via PL and TRPL measurements are shown in Figure 2-1 [5]. A more thorough discussion of the applications of each of these measurement techniques is beyond the scope of this thesis, but it is important to note that they both have the advantage of being rapid, non-contact, and can provide a wide range of insights to optimize a PV device.

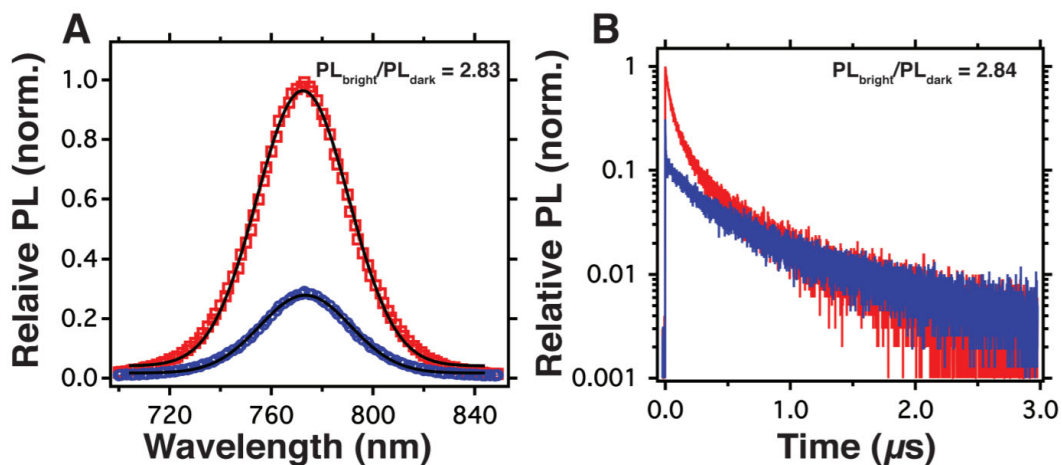


Figure 2-1: Examples of (A) PL and (B) TRPL spectra at two distinct regions of a $\text{CH}_3\text{NH}_3\text{PbI}_3(\text{Cl})$ film (shown in red and blue). This figure has been reproduced from its source [5].

2.3 Previous Work

The opportunity to develop characterization tools that advance beyond the existing state-of-the-art was identified by the GridEdge Solar Research program several years prior to the completion of this thesis. Therefore, it is important to note existing work that had been completed prior to the development of the most recent prototype. In summary, previous efforts had led to the fabrication of an initial prototype that later served as a proof-of-concept for demonstrating the ability to collect characterization data with a moving optical probe head. An image of the first tool iteration is shown in Figure 2-2.

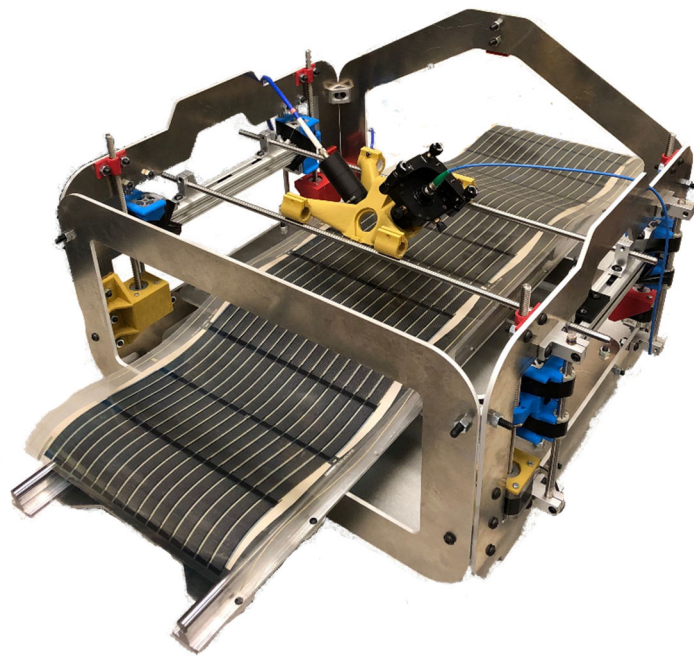


Figure 2-2: Image of an initial characterization tool prototype completed by the GridEdge Solar Research team in January 2020. This prototype was designed and built prior to the completion of this thesis and served as a vital proof-of-concept of the operating principles later refined in the final tool design.

This first design iteration was a foundational step in proving the feasibility of a large-format, optical characterization tool. Most notably, the optical probe head proved capable of collecting meaningful data with good signal-to-noise ratios. This achievement helped establish the data collection approach and mechanical architecture (i.e. optical measurements via a mobile probe head) later pursued in this thesis.

3. Solution Approach

3.1 Design Goals

Existing characterization equipment offers three categories for improvement that can lead to greater testing throughput and ultimately increase the pace of PV research. These categories include (1) reducing machine setup frequency, (2) decreasing human interaction time, and (3) allowing for rapid adoption of various characterization approaches. These points of consideration were directly translated into design goals for this research and are summarized in Table 3-1. It should be noted that these goals are specifically focused on addressing shortcomings of existing characterization solutions and do not represent a comprehensive list of design requirements which were later defined when developing particular subcomponents of the tool.

Design Goal	Proposed Solution Approach
Reduce machine setup frequency	Provide a sample tray that can accommodate at least 1 batch of samples in a single setup cycle. Assume a batch consists of 16 1” square samples.
Decrease human interaction time	Allow for automated interpolation of measurement instruments across all samples loaded into the tool. Ensure data collection software can store and consolidate testing results for each characterized sample.
Allow for rapid adoption of various characterization approaches	Devise a modular optics mounting probe that can be quickly replaced and readily modified to include a variety of lenses, objectives, and any other related optical components needed for signal transmission that novel characterization techniques may necessitate.

Table 3-1: A summary of critical design objectives and the performance metrics used to determine whether the proposed solution adequately improved on the current state-of-the-art.

In traditional PV characterization methods, many machines are often used to investigate different material properties of a given sample. These machine often have limited capacity and may require repeated sample loading in order to test a large batch of samples. Based on this reasoning, a key goal of the new tool design was to allow for multiple types of measurements to be completed simultaneously while also providing capacity to test a large batch of samples at once. This also resulted in a need for a modular optics mounting solution so that various light sources and detection equipment could be used in parallel or series during data collection.

Another drawback of existing characterization tools is the amount of time they require from research staff. In traditional methods, researchers often need to manually align and position optics relative to a sample they are interested in testing. This task requires the researcher's full attention and can be rather repetitive and tedious when examining a large batch of samples. In an ideal workflow, a sample tray full of devices would be loaded into the tool, the tool would be quickly calibrated, and the researcher would work on other productive tasks while the tool is collecting and organizing the data of interest. Therefore, a key goal for the improved tool design was to include an automated approach to data collection. From a mechanical design perspective, this meant that the optical probe head would need to be positioned through a motor-controlled motion platform.

The final point of consideration in determining design goals for the proposed tool was the ability to rapidly adapt to various characterization techniques. When considering less mature PV architectures, such as perovskites, it is important to note that the mechanisms driving device performance are still in the process of being discovered. As such, new material properties of interest (and techniques for investigating these properties) continue to be introduced to the field. To anticipate these changes and offer flexibility for diverse research efforts, a goal of the tools design was to incorporate modularity and the ability to rapidly expand testing capabilities as required by developments in the PV industry.

3.2 Operating Principles

The design goals of this project were ultimately distilled into a tool architecture that leverages insights provided from the existing proof-of-concept prototype previously shown in Figure 2-1. The chosen solution utilizes a mobile optical probe head that houses components for contactless characterization across an industry-standard A4 (297mm x 210 mm) sample tray. To conduct characterization test, external light sources are carried into the probe head and directed towards a sample. The resulting signal is then carried back out from the probe head to detection equipment. The probe head can then be repositioned to a new location to continue capturing data. Figure 3-1 illustrates the configuration of the tool's subcomponents and the high-level process flow by which the tool operates. The three main subcomponents of the tool – the light source, probe head, and detection equipment – are each designed for modularity and adaptability so they can be incorporated into a wide array of data acquisition techniques. Further explanation of these systems

and their specific process flows is described below, starting from the light source, to the optical fiber, to the probe head, to signal collection through another optical fiber, and finally to the detection equipment.

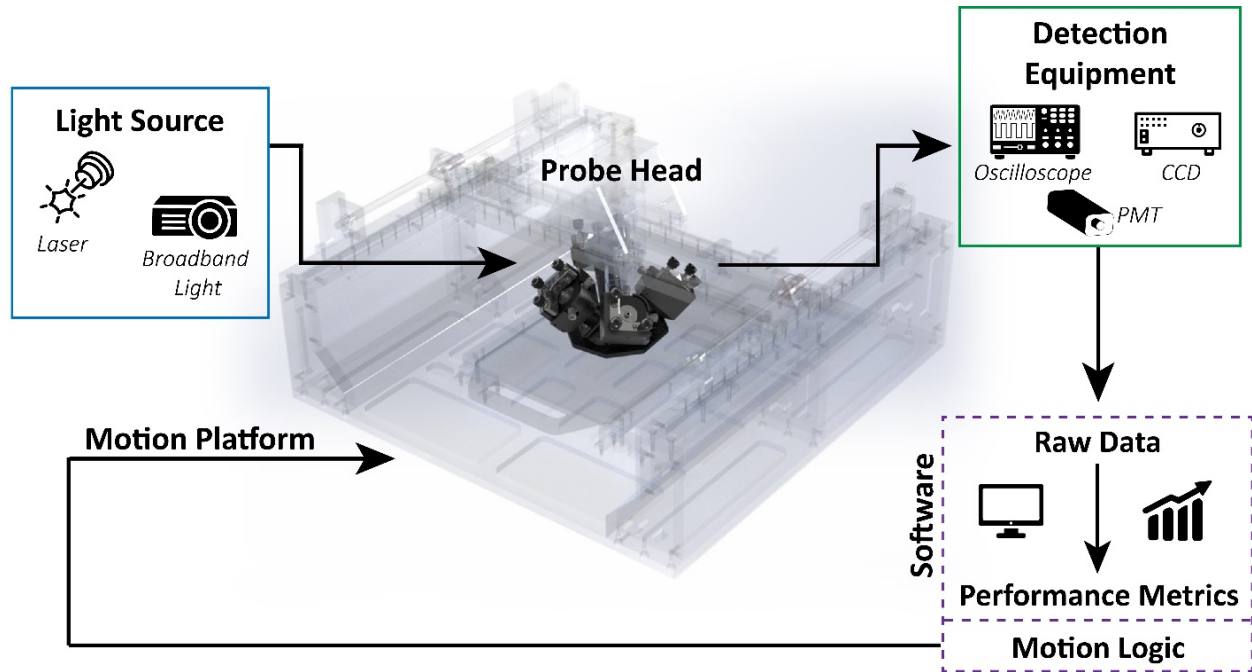


Figure 3-1: Rendering of the current optical characterization tool design with the critical subcomponents and the process flow between them labeled.

The light source can vary depending on the tool’s application and multiple light sources can be used simultaneously. For example, a monochromatic light source, such as a laser, could be used alongside a broadband light source such as a xenon arc, tungsten, or metal halide lamp. Any of these light sources could also be used independently if desired.

The light source is then transmitted to the optical probe head via an optical fiber. The optical fiber is selected based on characteristics such as appropriate signal attenuation, spectral window, and permitted optical modes depending on the measurement type. This further contributes to the overall flexibility of the tool since light sources and detection equipment can be placed externally from the tool. As a result, these external components can remain part of other optical systems a lab may actively use while still being utilized for this tool when needed. From a design perspective, this also enables considerable cost savings for research labs since existing capital equipment can be accommodated to operate with the tool.

As the light source enters the probe head, it is adjusted and focused to meet the needs of the testing application. The specific signal tuning requirements vary based on the light source, sample, and characterization tests being performed. The probe head accounts for the range of tuning needs through the implementation of a modular optics mounting strategy. All optics utilize industry-standard threading for easy interchangeability. This enables a variety of optical components – such as lenses, lens tubes, and light filters – to be placed between the input optical fiber and the sample. The modularity of optical components also applies to the collection optics which collect and filter the signal from the sample and relay it through an output optical fiber.

The output optical fiber can carry the signal to a variety of detection systems. These systems are necessary intermediaries that allow signal from the sample to be interpreted into meaningful data. Detection systems can include devices such as a single photon avalanche photodiode (SP-APD), a photo-multiplier tube (PMT), a charged coupled device (CCD), and/or an oscilloscope. Modular software design allows for code wrappers to be integrated into the tool's main software that are capable of translating and controlling detection equipment through their native software library. As a result, the characterization tool can be made compatible with a wide range of detection equipment models and manufacturers.

To summarize, the proposed tool design operates on the principle of using a mobile optical probe head that directs signal to and from a sample in a variety of configurations that correspond to various standard optical characterization techniques. From a mechanical design perspective, the two critical subcomponents that required development in order to bring this solution to fruition included the optical probe head – where all of the optics mount – and the motion platform – which is responsible for positioning the probe head relative to samples.

4. Optical Probe Head Assembly

4.1 Purpose & Requirements

Prior to detailing the design efforts involved in developing the optical probe head assembly, it is important to explain its purpose and the performance requirements it needed to meet. The optical probe head is intended to serve as the central component of the optical characterization tool, relaying signals to and from a sample during measurement. In returning to the overarching design goals for the tool outlined in Table 3-1, the design of the probe head assembly needed to support efforts to reduce machine setup frequency, decrease human intervention, and offer modularity to accommodate a wide variety of characterization techniques. These goals were concentrated into specific design requirements for the probe head assembly listed in Table 4-1. Note that this table defines metrics of success for each requirement which were referenced when formulating a design solution and also served as a basis for evaluating the final design.

Requirement #	Requirement Description	Metric for Success
4-1.1	Accommodate multiple illumination and collection optics simultaneously.	Include a minimum of 4 mounting locations for optical assemblies.
4-1.2	Provide localized light shielding to reduce signal noise.	Achieve data collection with a low signal-to-noise ratio in a room with ambient lighting.
4-1.3	Provide a rigid mounting point for optics assemblies.	Allow a maximum deflection for optical assemblies of 100 μm . This is assumed to be within the range of alignment adjustments that can be made during initial optics alignment.
4-1.4	Allow mounting to a motion platform so the probe head can be positioned relative to an A4 side sample tray.	Provide a mounting surface that does not impede optics paths.
4-1.5	Allow for a wide variety of lens configurations that different measurements may require for light tuning and filtering.	Ensure compatibility with industry-standard optical components.
4-1.6	Enable adjustable alignment of optics assemblies.	Provide adjustment for incoming optical fibers in 5 degrees-of-freedom at magnitudes that overcome potential manufacturing inaccuracies.

Table 4-1: Design requirements table for the optical probe head assembly

The resulting solution for the probe head assembly includes two key components that were designed to directly satisfy the requirements listed in Table 4-1. The first is the probe head itself, which links optical components and the motion platform that positions the probe head. The second is a kinematic mount coupling which provides a means for aligning signals exiting or entering a given optical fiber while maintaining compatibility with off-the-shelf optical components.

4.2 Probe Head

The final probe head design is shown in Figure 4-1. Many of its core design features remained unchanged from the initial prototype developed prior to the completion of this thesis (see Figure 2-2). The most notable feature that carried over into the final design is the configuration of four optics mounting locations that are directed at a single focal point. A discussion of the probe head's critical design elements and their relationship to the requirements outlined in Table 4-1 are discussed below.



Figure 4-1: Rendering of the optical probe head assembly with the probe head labeled. The optics are displayed semi-transparent to more easily identify the probe head.

As noted, the final probe head design includes four mounting points for lens stacks which place illumination and detection optics equidistant at complementary angles so that each optical configuration shares the same focal point. The incorporation of multiple mounting points for

illumination and collection optics gives the tool the capability of collecting a combination of data simultaneously (Req. 4-1.1). This not only increases throughput: it also allows for the application of device models that can process multiple data types. Figure 4-2 shows an example of a probe head configuration that transmits input signal through one set of illumination optics and collects a samples excited response via two separate collection optics assemblies. The signal collected by each collection assembly is functionally equivalent due to the Lambertian emission profile transmitted from the excited sample. A Lambertian emitter is defined as an areal element in which the radiance of light scattered towards an observer is independent of the observation direction and the radiant intensity of that light is also proportional to the cosine of the angle between the observation direction and the surface normal, as illustrated in Figure 4-3 [6]. This property ultimately enables each collection assembly to receive the same signal – despite their different locations – and independently tune, filter, and transmit it out to separate detectors required for measuring different material properties simultaneously.

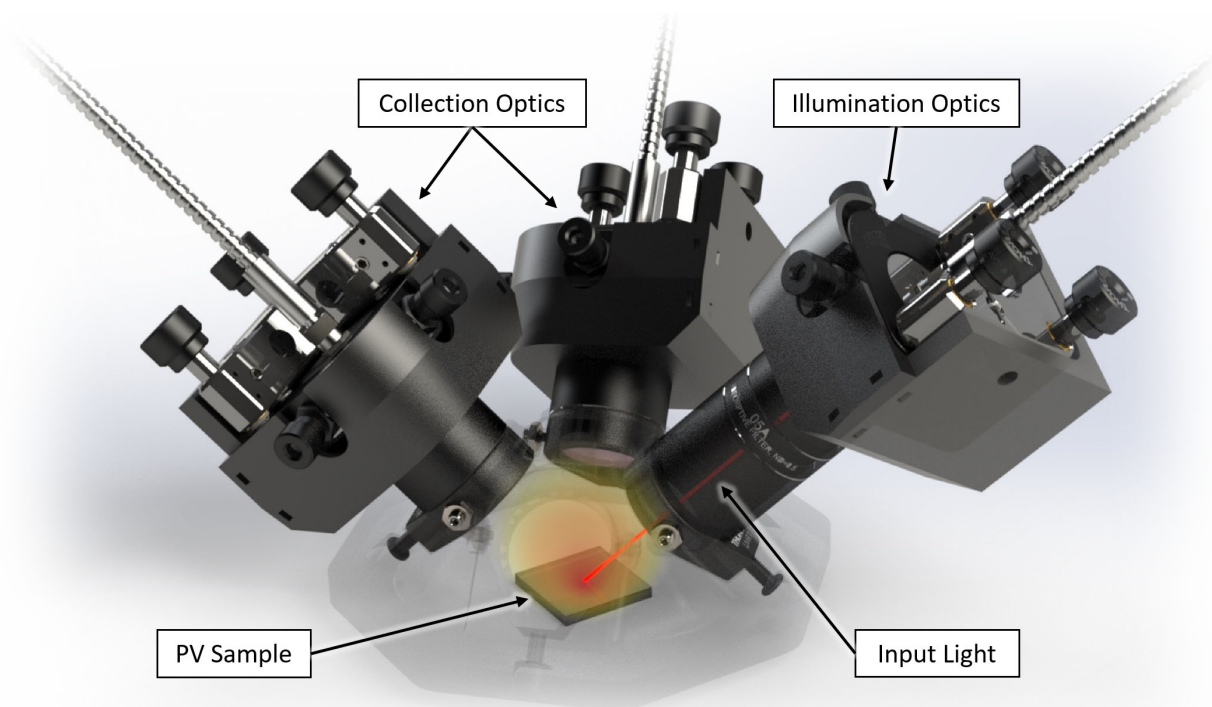


Figure 4-2: An optics configuration using one set of illumination optics and two collection optics assemblies. The input light is shown exciting a sample. The Lambertian emission generated by this excitement is then equivalently captured by each collection optics assembly and independently tuned, filtered, and transmitted back to specific detection equipment necessitated by the material property being measured.

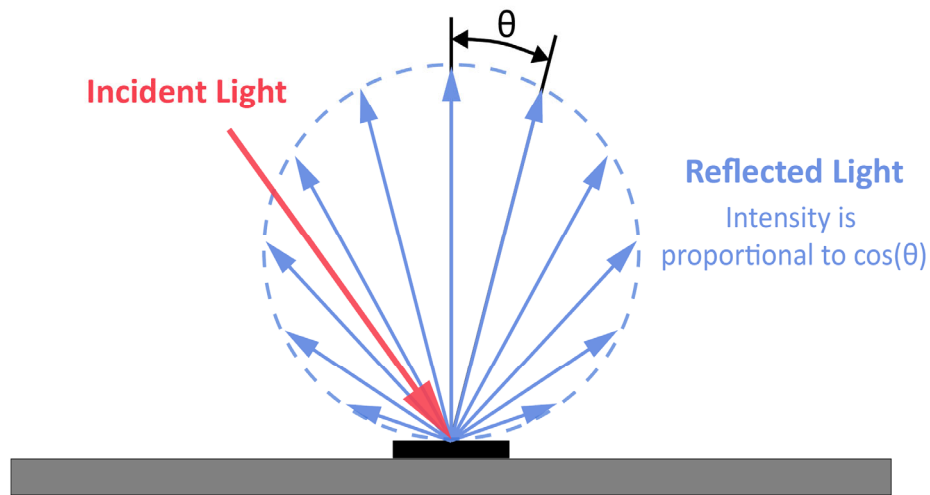


Figure 4-3: A 2D representation of a Lambertian emitter. Incident light is equivalently radiated independent of the observation direction. The radiant intensity is proportional to the cosine of the angle between the observation direction and the surface normal.

The shared focal point of each optics assembly is located just below the base of the probe head in order to avoid collision with the sample while still shielding external light that would impact the signal-to-noise ratio (Req. 4-1.2). This configuration allows for collection of reflected light as well as emission. Future embodiments of this tool could collect sample signals at oblique angles to quantify light directionality. This data can either be spatially or spectrally filtered to avoid signal cross-talk along different points of the optical train.

The optical probe head is also designed to serve as a rigid mounting point for each optics assembly (Req. 4-1.3). Optical characterization techniques are sensitive to variations in signal alignment, so a robust connection between the optics assemblies and the probe head is imperative. Previous design iterations relied on a single bolted connection that joined the lens stack to the probe head. This approach proved unstable and was ultimately addressed by adding two additional clamping points at the top the lens stack connection, as shown in Figure 4-4. The additional clamping surfaces relieved the torque placed at the bottom of the lens stack that resulted from the weight of the cantilevered optics assemblies. The probe head was also designed to be 3D printed, which raised potential concerns for the rigidity of its construction. Finite Element Analysis (FEA) was conducted to analyze this concern. Four 50 mm lens stacks were placed on the model to simulate a worst-case loading condition. The resulting analysis, shown in Figure 4-5, resulted in a maximum local deflection at the optics interfaces of about 30 μm , assuming the probe head were to be 3D printed with polylactic acid (PLA). While a maximum allowable deflection had not been

previously defined, this relatively low value was insufficient to warrant further concern and 3D printing with PLA proved to be the most convenient fabrication method.

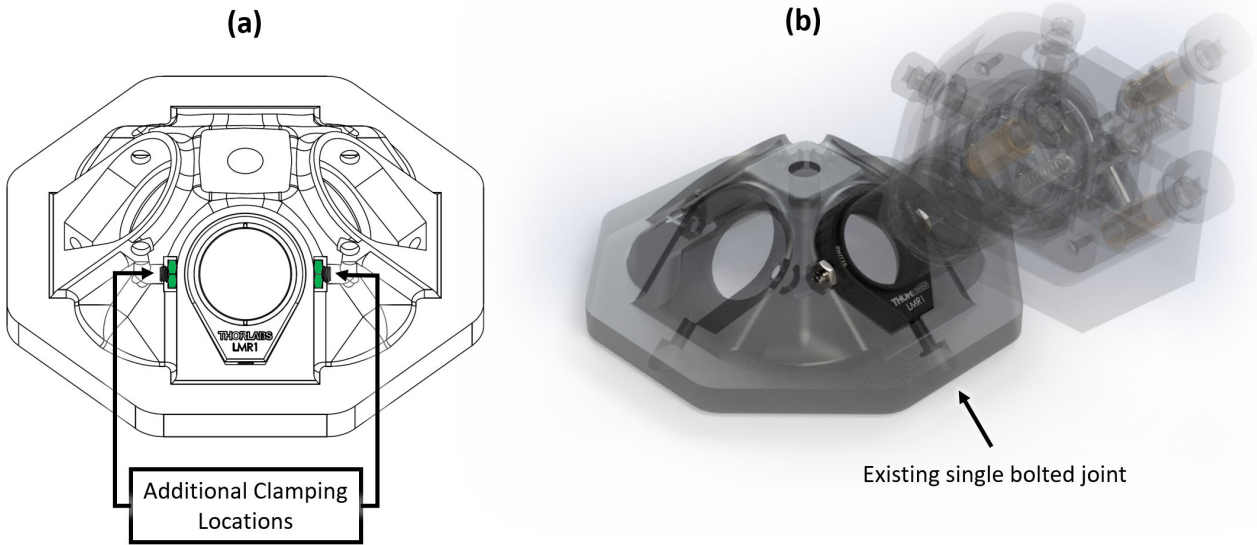


Figure 4-4: (a) An engineering drawing showing the location of additional set screws added to the probe head for clamping optics assemblies. (b) A rendering showing the same added set screws as well as the existing bolted joint that previously served as the only fastening point for the optics.

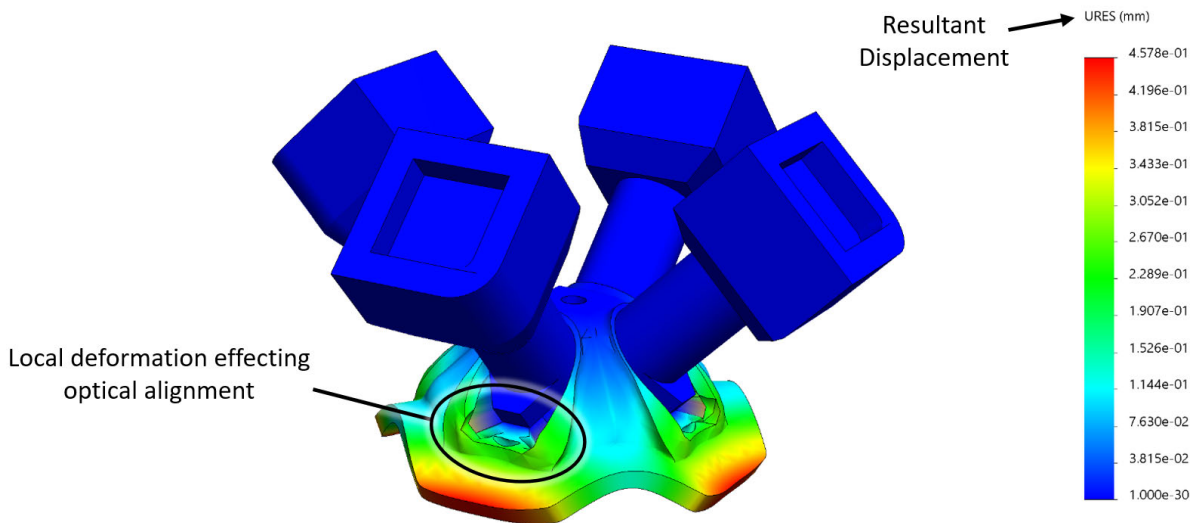


Figure 4-5: FEA results for the optical probe head with 4 large optics assemblies mounted. The simulation assumes the probe head is constructed of PLA and is under static load from the mass of the optics. The maximum global deflection recorded is 46 μm . The maximum local deflection expected at the optics assemblies (circled) is lower, at about 30 μm . Given the low magnitude of deflection, PLA was deemed a sufficient material for the probe head.

In order to position the probe head, a mechanical interface connecting to the motion platform also needed to be designed (Req. 4-1.4). This was readily achieved through a bolted connection which joined the probe head to a column suspended from the motion platform. In the initial embodiment of this solution the suspended column was a uniform shaft with threads tapped on both of its faces. During assembly and testing, this proved to be inconvenient to users because the bolts on either end of the shaft were difficult to reach. A quick design revision resulted in a two-part column that made removing and attaching the probe head a much easier task. This revision also further supported the overall goals of the tool to save researchers time and support rapid adoption of different characterization techniques since the probe head was now “hot-swappable”.

The process of attaching optics to the probe head was also designed to be completed with relative ease (Req. 4-1.5). The mounting point of the optics assembly (previously shown in Figure 4-4) was made to accommodate a standard 1” lens mount. This meant that any common 1” lens, lens tube, or filter could be readily incorporated into both the illumination and collection optics assemblies. Figure 4-6 provides an example of a potential probe head configuration that includes illumination and collection optics with varying lens assemblies.



Figure 3-6: An exploded view of an example configuration of the optical probe head. Signal is transmitted to the kinematic mounts via optical fibers. That signal is then aligned via the kinematic mount and coupling assembly so that the light can be filtered and tuned as it is directed to and from a sample.

4.3 Kinematic Mount Coupling

While the probe head allows for fixed mounting of optical components, a separate kinematic mount coupling needed to be designed in order to enable adjustment when aligning the input and output optical fibers (Req. 4-1.6). The kinematic mount coupling threads directly to the optics assemblies at the opposite end of the probe head, as shown in Figure 4-7. A vendor-supplied kinematic mount is then fixed to the coupling where the fiber port is attached with clearance for adjustment of the fiber. The kinematic mount is attached in such a manner that the optical fiber can be adjusted in five degrees-of-freedom (DOF) independently from the fixed optical components that are attached directly to the probe head. This is crucial for calibrating optics and correcting for manufacturing inaccuracies. A light shield was also added to the kinematic mount coupling in order to prevent ambient light from generating noisy data (Req. 4-1.2).

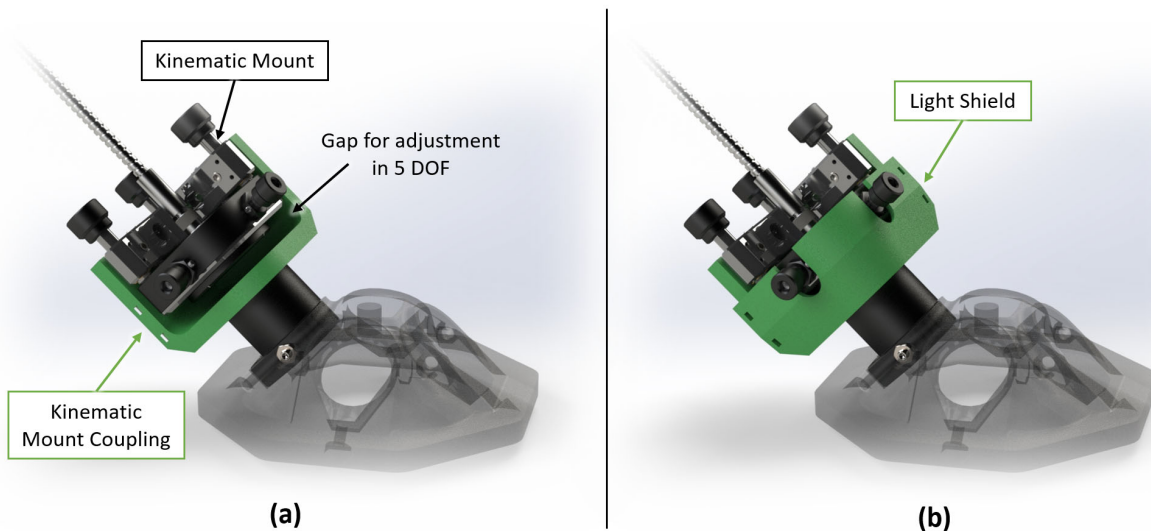


Figure 4-7: A closer view of the kinematic mount coupling with the light shield (a) removed and (b) attached. The kinematic mount coupling serves as an intermediary connection between the kinematic mount, where the optical fiber port enters, and the lens stack. The coupling provides adjustment of the optical fiber in 5 degrees-of-freedom (DOF) so that signals entering and exiting the probe head can be adjusted and aligned for accurate data collection.

Just as with the probe head, rigidity of the kinematic mount coupling was particularly concerning since it is directly responsible for signal alignment and was originally intended to be manufactured via 3D printing. Given the relatively simple geometry of the part, FEA was not performed since it was determined that the coupling could be machined with aluminum or steel if greater rigidity was required after testing.

5. Motion Platform

5.1 Purpose & Requirements

The motion platform is responsible for positioning the optical probe head within the tool. A critical goal defined at the start of this project was to include an autonomous system for collecting data (see Table 3-1). As a result, the motion platform needed to be actively driven by motors that could traverse the sample tray and ensure data was collected at precise locations on a given sample as defined by a researcher’s requirements. The motion platform also has significant impacts on the overall architecture of the tool and the way in which it operates. To organize the performance specifications that the motion platform would need to achieve, design requirements were specified are shown in Table 5-1. This table reflects many of the same qualities as the requirements previously outlined for the optical probe head (see Table 4-1) and again served to guide the design process and provide a benchmark for determining the success of the final design.

Requirement #	Requirement Description	Metric for Success
5-1.1	Isolate motion to only involve the probe head (i.e. keep the sample tray stationary) to demonstrate potential applications on a manufacturing line.	Achieve positioning of the probe head in a three-dimensional work envelope through motion of the probe head alone.
5-1.2	Maintain a relatively compact footprint that does not exceed a footprint of 24” x 24” .	Measure the area of the tool’s base to ensure it does not exceed 24” x 24”.
5-1.3	Limit the weight of the tool to a maximum of 65 pounds.	Achieve a final weight under 65 pounds. This limit does not include the optical probe head assembly, which can be assumed to be removed when moving the tool.
5-1.4	Provide repeatable positioning and motion resolution on the scale of 10’s of microns.	Empirically measure the minimum incremental motion (MIM) of the probe head and compare it to the maximum allowable value of 10 μ m.
5-1.5	Achieve minimum linear motion speeds of 3 m/s.	Empirically record the traveling speed of the probe head to verify if it meets the minimum criteria.

Table 5-1: Design requirements table for the optical probe head assembly

With requirements in place, the motion platform was divided into two critical categories. The first was the actual designed components that comprise the physical architecture and mechanics of the tool. The second was vendor-supplied components such as the motors, lead screws, and linear rails which were specified to match the unique needs of the optical characterization tool.

5.2 Tool Architecture

A wide variety of machine architectures were considered when designing the motion platform of the optical characterization tool. One of the first fundamental considerations was determining whether to use a traditional Cartesian based system or a free-form robotic arm. Each approach had the potential to satisfy the design requirements laid out in Table 5-1, but a Cartesian system was chosen based on its relative simplicity. The next challenge was determining how to configure the linear actuators that would provide motion in each Cartesian axis. After surveying the structures of existing machines with comparable positioning functionalities – such as 3D printers and coordinate measuring machines (CMM's) – a gantry system was chosen, as shown in Figure 5-1. Machine coordinates are also labeled in the figure for future reference.

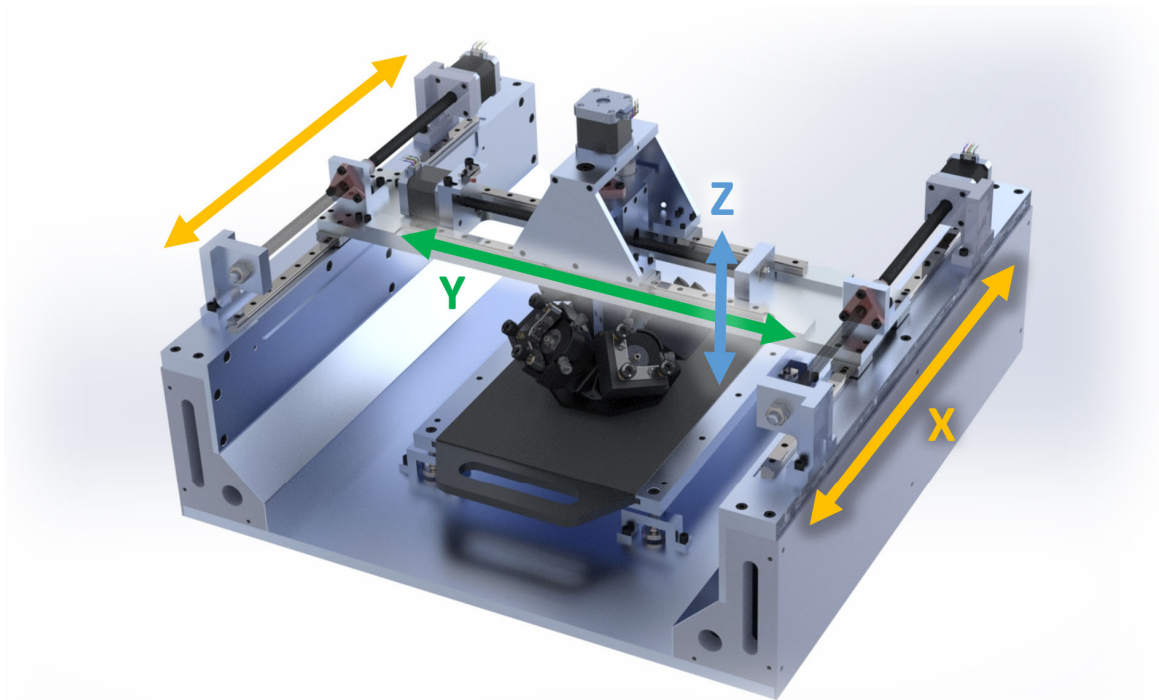


Figure 5-1: Rendering of the characterization tool with each motion axis labeled. The tool utilizes a gantry-based motion architecture commonly found in tools with similar positioning requirements such as 3D printers and coordinate measuring machines (CMM's).

The gantry system structure is ideal since it enables the sample tray to remain stationary (Req. 5-1.1). This gives the optical characterization tool (which has been designed specifically for use in a research lab) the opportunity to also demonstrate potential applications in manufacturing environments. If an optical probe head were to be incorporated onto a PV manufacturing line to record measurements for process control, its motion would most likely need to be separate from that of the manufacturing line itself. Therefore, it was advantageous to isolate the optical probe head as the only element that would translate as the machine positioned the optics over a sample, even in a tool strictly designed for lab use.

The motion architecture also needed to maintain a feasible size and weight so that it could be placed within an optics lab and be safely moved as needed. The final volume of the tool is labeled in Figure 5-2. The resulting footprint matches the maximum allowable requirement of 24" x 24" (Req. 5-1.2). Achieving this result took careful consideration given the size of the sample tray and need to maintain space for the probe head and optical fibers feeding in and out of it.

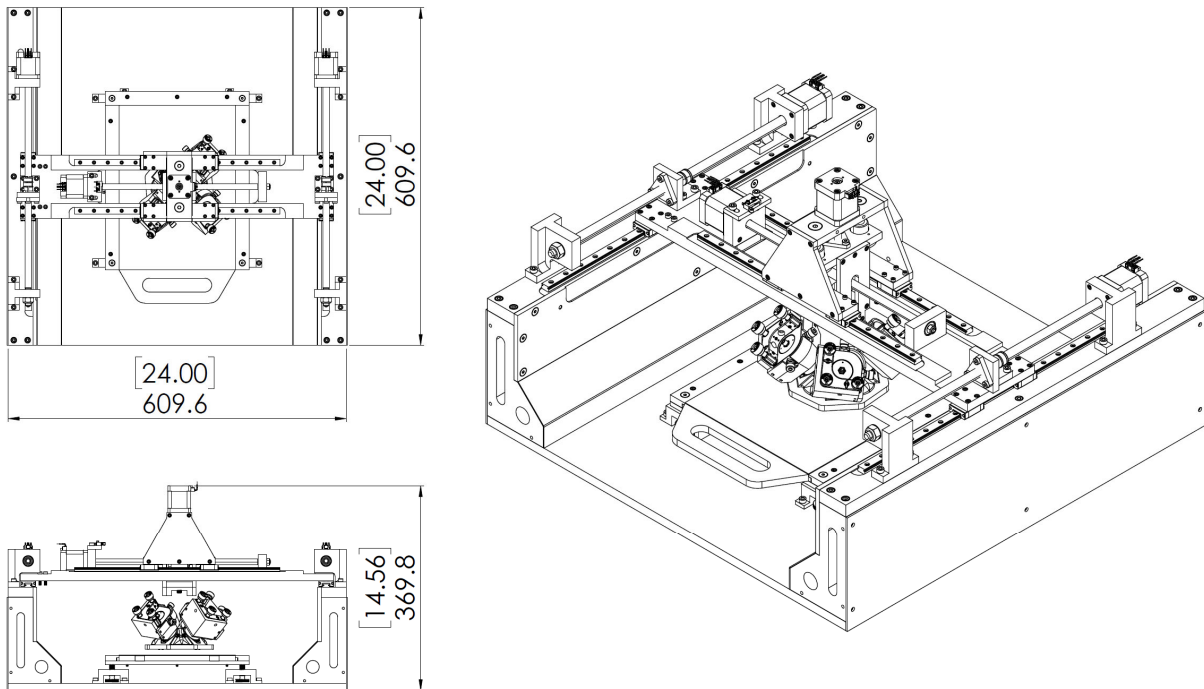


Figure 4-2: Drawings of the optical characterization tool prototype with the overall volume labeled. The footprint of the tool meets the upper bound of the 24" x 24" limit (Req. 5-1.2). The height of the tool is similarly constrained to ensure it does not consume excessive space when deployed in a research laboratory.

The tool was also designed to be lifted by two people in the case that users would want to relocate the machine without any specialized handling equipment (Req. 5-1.3). The United States Occupational Safety and Health Administration (OSHA) recommends an individual lifts no more than 50 pounds when handling items in a work environment [7]. This suggestion served as a baseline in determining a maximum allowable weight for the tool of 65 pounds (based on the assumption that one individual may bear upwards of 75% of the tools weight when lifting with a partner). Achieving this target weight while maintaining a rigid machine structure required several design iterations. The final design includes multiple components with weight-relief features intended to be machined away from part elements that would not impact the overall structure of the tool. An example is shown in the engineering drawings for the tools base plate shown in Figure 5-3. This component is machined from MIC6 cast aluminum and the addition of relief pockets reduces the parts mass by 4.7 kg, leaving the resulting part at just 63% of its original mass.

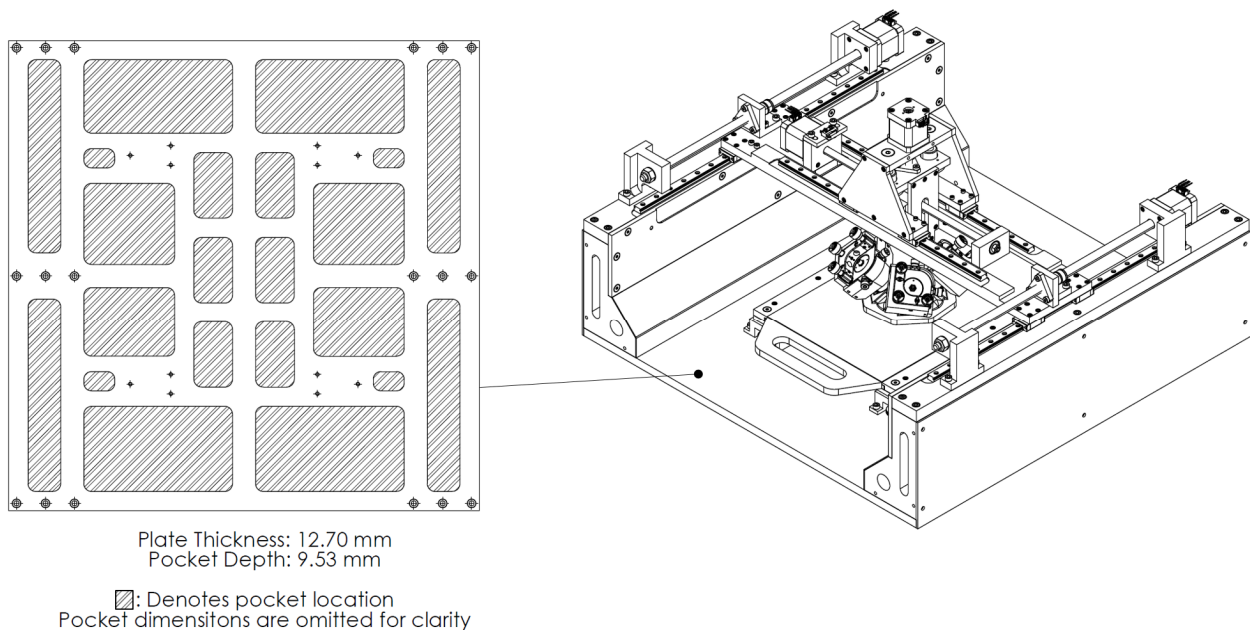


Figure 5-3: Drawing of weight-reduction pockets included in the design of the tools base plate. The inclusion of these pockets results in a 4.7 kg reduction in mass, to a final part mass that is 63% of the original design without the pockets included.

As was previously noted, the rigidity of the tools structure was a critical requirement. At the onset of the project, the goal was to provide positioning resolution and repeatability on the order of 10's of microns (Req. 5-1.4). This level of precision meant that each motion axes needed to be designed such that they were not susceptible to significant deflections while the tool operates. A focus was specifically placed on analyzing the axis spanning the gantry since its loading conditions

were the most unfavorable of the three Cartesian axes. Figure 5-4 captures the FEA that was performed in the final iteration of this component. The simulation provided a maximum expected deflection of 13.8 μm . Note that this is an overestimate since the loading conditions applied via the mass of the z-axis and optical probe head assemblies were simplified to point loads centered at the middle of the gantry span. Despite the overestimation, a 13.8 μm deflection is within a permissible range of the positioning resolution requirements for the tool. Notice that weight reduction pockets were also included in the design of the gantry cross member. As the cross-section in Figure 5-5 demonstrates, these pocket allowed a 17.5% reduction in mass while reducing the area moment of inertia of the part by nearly an equivalent 17.3%. This is one of many examples where the tradeoff between mass and performance of specific parts was considered. In this case, the extra pockets were included since the y-axis gantry cross-member achieved permissible deflections (see Figure 5-4) while reducing the overall tool mass and decreasing the load the x-axis motors would need to drive.

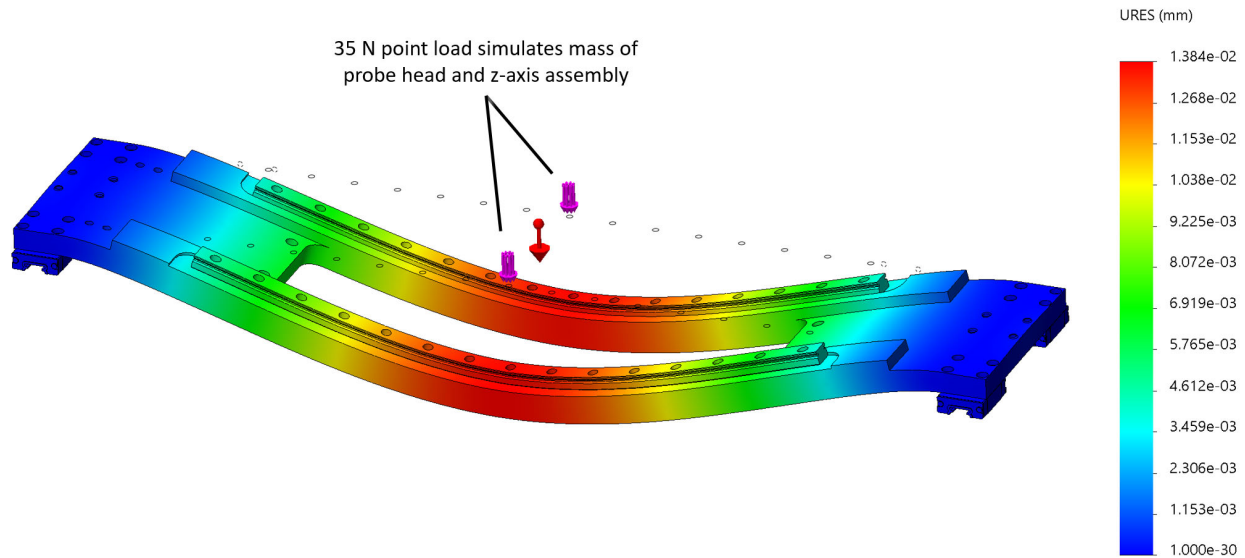


Figure 5-4: FEA of the y-axis gantry cross-member. The simulation assumes the cross-member is comprised of 6061 aluminum alloy with 316 stainless steel linear rails attached. The maximum calculated deflection is 13.8 μm . This is an overestimate since the loading conditions (from the mass of the probe head and z-axis assembly) have been simplified to point loads at the center of the gantry whereas this load is distributed over a larger area on rail carriages in practice.

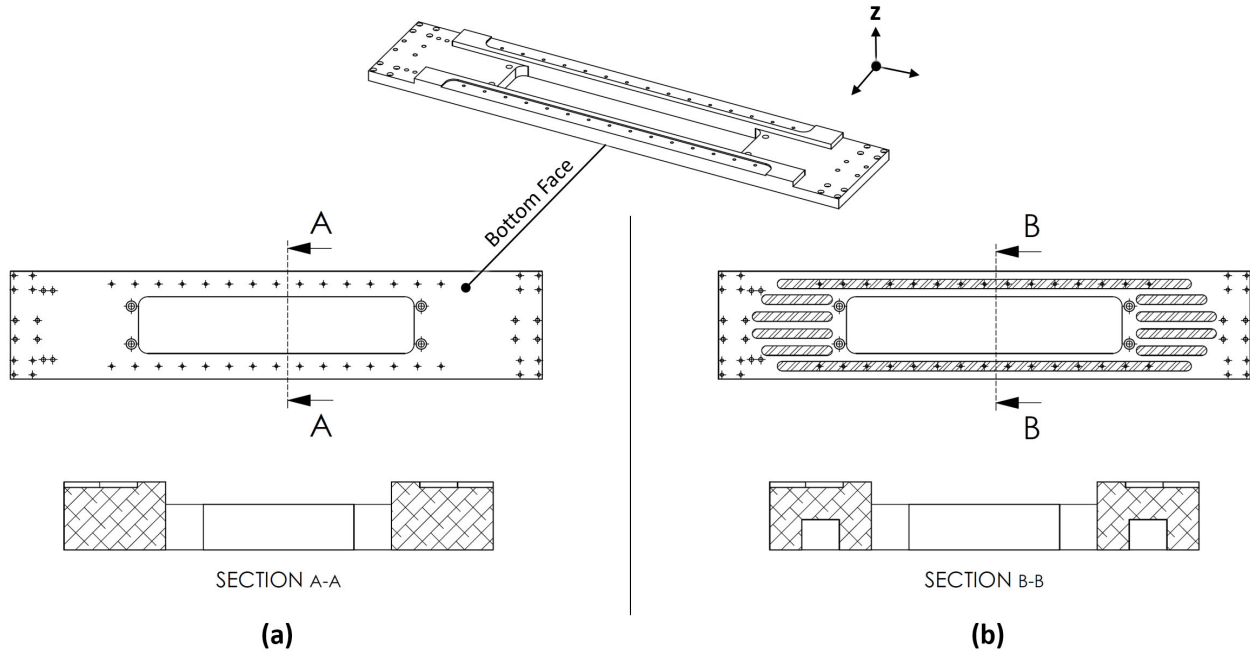


Figure 5-5: Cross-section views of the x-axis gantry cross member (a) before and (b) after the addition weight-reduction pockets. These pockets enable a 17.5% reduction in mass while also causing a 17.3% decrease in area moment of inertia. The deflection analysis in Figure 5-4 verified that the maximum deflection after adding these pockets was permissible.

5.3 Motion Components

Vendor-supplied components were also an important consideration when designing the optical characterization tool. These components largely focused on the dynamics involved in positioning the optical probe head assembly. Given the need for relatively high precision motion control (potentially on the order of 10’s of microns for imaging-based characterization; Req. 1-5.4), a lead screw and stepper motor assembly were chosen for power transmission.

The process of determining which linear motion components to source started with calculations focused on the lead screw and motor. The first consideration was determining the desired lead (linear distance traveled per revolution) of the lead screw. Since a motion resolution on the order of 10’s of microns was required, the lead screw assembly needed a minimal incremental motion (MIM) below this threshold. Using Equation 1, and assuming the stepper motor paired with the lead screw would be direct-drive and operate at an industry-standard 200 steps per revolution, a lead of 1 mm was determined to be ideal since this would provide an MIM of 5 microns. Note that this resolution requirement holds for all three Cartesian axes, so all lead

screws within the machine required a 1 mm lead. Another consideration when selecting lead screws was the diameter of the screw. As a best practice, it was determined that the lead screw with the largest diameter that met the 1 mm lead requirement and could be readily sourced would be chosen.

$$MIM = Lead \left[\frac{mm}{rev} \right] \times Stepper \text{ Resoluton} \left[\frac{rev}{step} \right] \quad (1)$$

After considering many lead screw suppliers and evaluating several motor and lead screw coupling strategies, it became apparent that an integrated motor and screw assembly would provide an ideal form-factor. In both the z- and y- axes, the additional assembly length needed to mount a shaft coupling would have required these axes to become longer, adding undesired mass and potentially forcing the tool to exceed its volume requirements (Req. 5-1.2). Thus, an integrated motor and screw assembly was the most desirable option since no additional coupling mechanism was required. After evaluating suppliers, customized motor and lead screw assemblies were sourced from PBC Linear. Note that the motor torque-speed curve was also considered when choosing the motor-lead assembly. Equations 2 and 3 were used to estimate the maximum drive torque any motors within the tool would experience and the corresponding linear speed at this load.

$$Torque_{Drive} = \frac{Load \times Lead}{2\pi \times Efficiency} \quad (2)$$

$$Linear \text{ Speed} = Lead \times RPM \quad (3)$$

Using the torque-speed curve shown in Figure 5-6 and an efficiency of 18% given by the lead screw supplier [8], the maximum drive torque expected within the tool (along the y-axis) was equal to 30.9 mNm. Since the load is relatively small, the motors were expected to operate at maximum rotational speeds (1800 RPM for a 24-volt configuration), which corresponds to a maximum linear speed of 0.3 m/s. This is well below the 3 m/sec requirement outlined in Table 1.5 (Req. 1.5.5), but a concession was made for the sake of positioning resolution. It may seem counterintuitive to sacrifice speed given the overall goal of the tool to increase the pace of PV research (see Table 1.3), but the additional time spent interpolating to new positions along the sample tray is incremental compared to the time required to perform measurements at each sample.

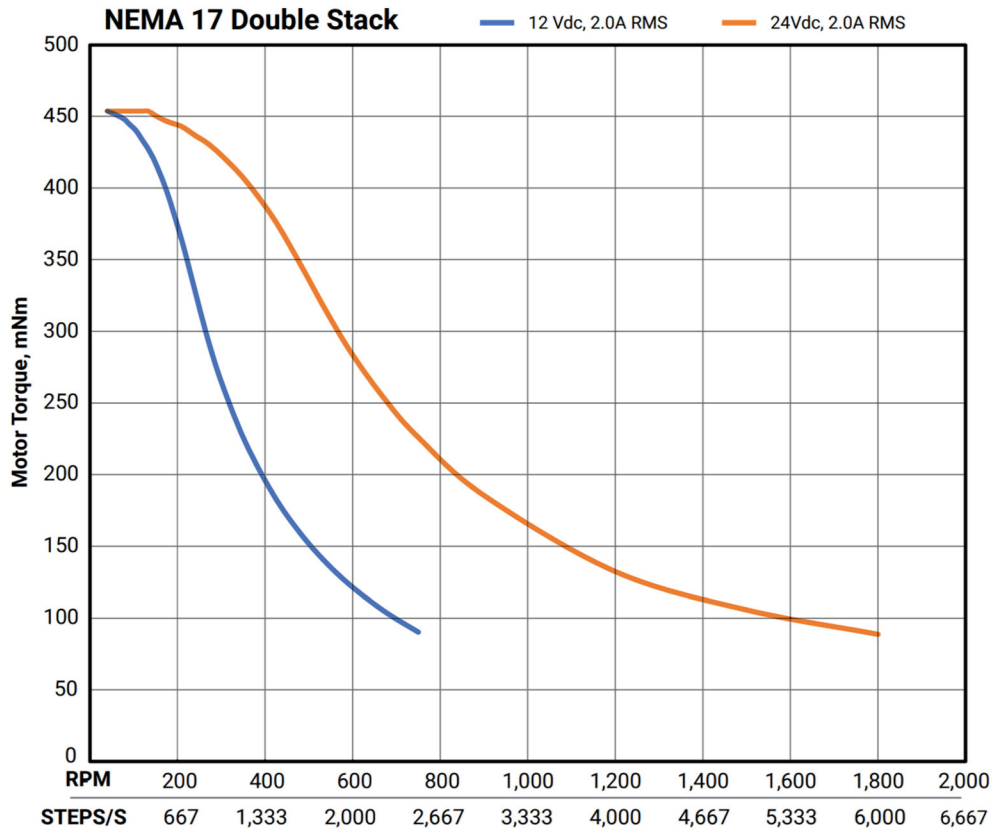


Figure 5-6: The torque-speed curve for the motors sourced for the optical characterization tool. The maximum drive torque expected within the machine was 30.9 mNm, so the motors were expected to operate at the maximum plotted speed of 1,800 RPM when powered by 24 volts. This figure is modified from its source [8].

5.4 Fabrication & Assembly

With the motion platform design complete, efforts shifted to fabricating parts and bringing the optical characterization tool concept to fruition. Due to the COVID-19 pandemic, access to machining resources were limited. As a result, all parts were manually machined on a personal Southwest K3 Sport knee mill. This meant that some part designs needed to undergo minor revision in order to make manual machining more feasible. For example, the weight reduction pockets intended for the tools base plate (and previously shown in Figure 5-3) were foregone due to time constraints. Nonetheless, all of the parts were capable of being manufactured to their intended functionality and were assembled for testing as shown in Figure 5-7.

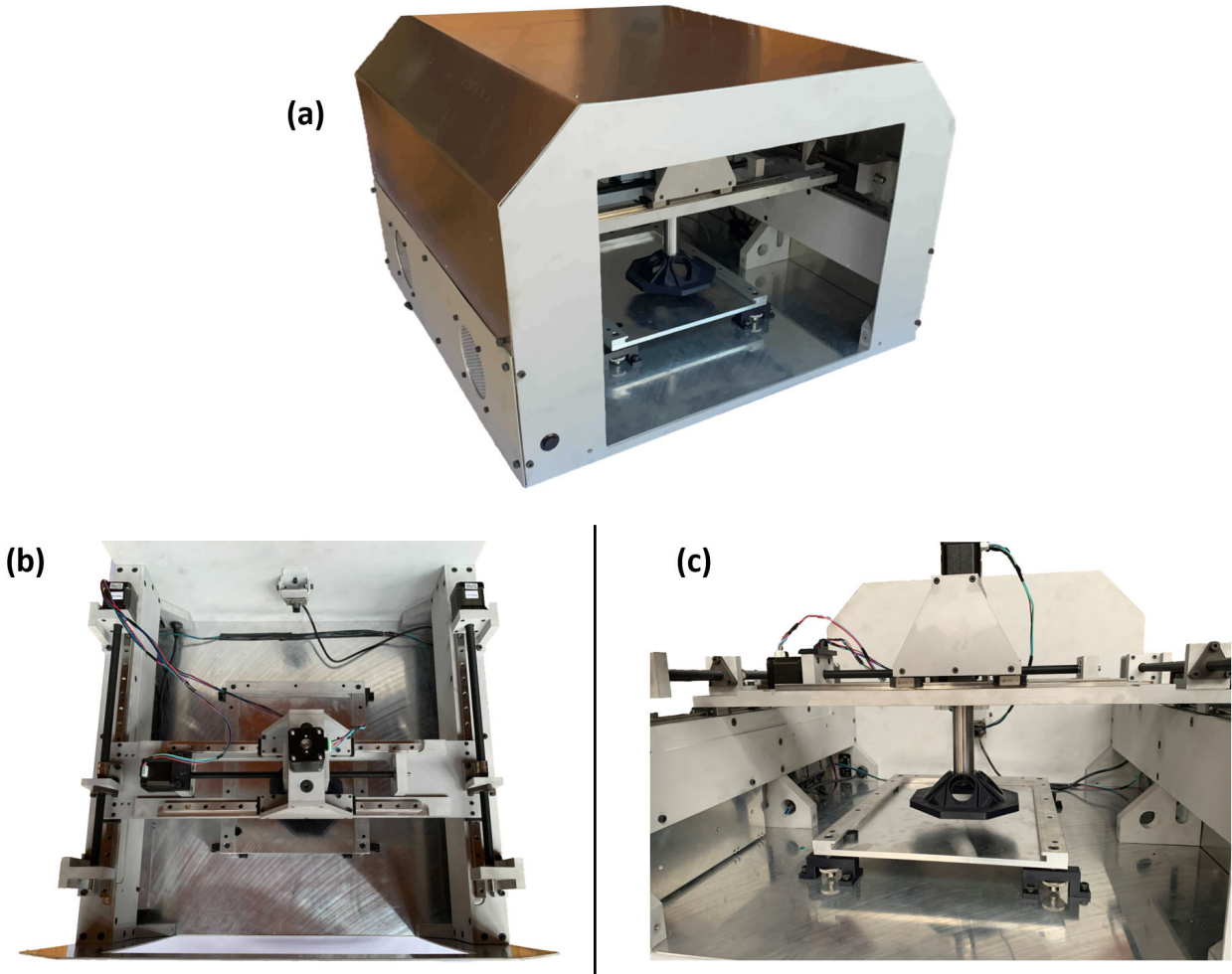


Figure 5-7: Images of the finalized optical characterization tool prototype (a) with the enclosure on, (b) from a top-down perspective, and (c) directed at the probe head and sample tray.

6. Design Evaluation

6.1 Sample Data Collection

While many design requirements were specified for specific features of the optical characterization tool (see Table 4-1 and Table 5-1), the most critical aspect of the tool's performance is whether it is capable of collecting meaningful data. Initial testing has confirmed that the tool is capable of collecting both steady-state PL and TRPL data, as shown in Figure 6-1. The tool has also proven capable of automated positioning over several sample locations that can be specified as needed by a researcher interested in collecting data for a batch of samples. These

achievements demonstrate that the tool design is capable of the desired high-level functionality. More specifically, multiple data types can be collected simultaneously, the process of collection is automated once samples are loaded, and the tool's optical probe head can be readily adjusted to accommodate various characterization techniques as required.

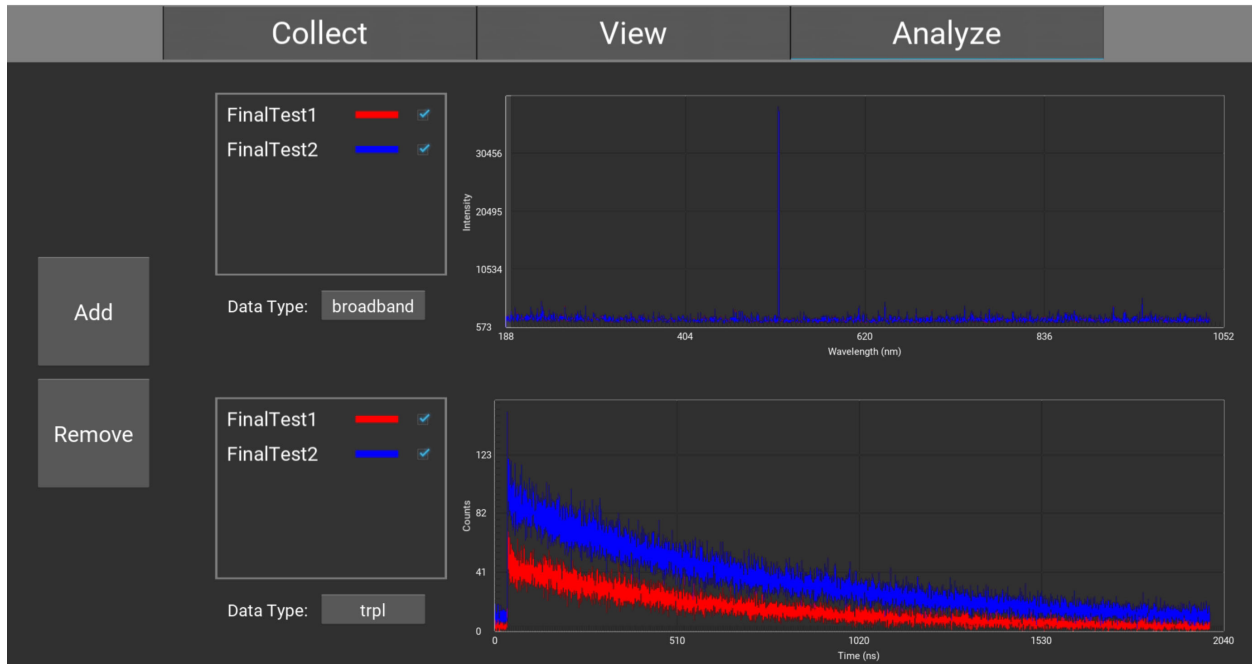


Figure 5-1: Sample steady-state PL (top) and TRPL (bottom) data collected at two locations with the tool prototype. The data collection process and creation of the shown plots was completed autonomously after inputting the sampling locations in the tool's software and selecting the desired tests to perform.

6.2 Shortcomings and Future Work

While the tool certainly achieves its overall design intentions, the specific design requirements outlined in Table 4-1 and Table 5-1 can be revisited to assess potential shortcomings and evaluate where to focus future efforts developing the tool.

Nearly all requirements for the for the optical probe head assembly from Table 4-1 have been met with the current tool design. Despite this, two areas for improvement are apparent. The first is reevaluating the tool design such that it can be more easily manufactured with materials with greater rigidity than 3D printed PLA. As previously noted (see Figure 4-5), initial FEA determined that PLA could exhibit deflections upwards of 46 μm during loading under unfavorable optics configurations. Changing the material from PLA to 6061 aluminum alloy and reevaluating the

FEA results leads to a 9.2% decrease in estimated deflection. This magnitude of reduced deflection may prove significant in future measurement applications that require greater precision and repeatability. The probe head assembly could also improve from revisions to the alignment mechanisms. Most notably, the current solution still relies on users to manually align optics when they are initially mounted to the probe head. Enabling automated alignment as a setup protocol to the tool will lead to faster data collection when switching probe head configurations and also ensure alignment is maintained and validated prior to each data collection cycle.

The motion platform offers several areas for improvement as well. The final prototype exceeded the mass requirement and ended up being cumbersome to position in lab. This could be readily addressed by remanufacturing parts, such as the base plate, to include the weight reduction pockets that were not machined in the current prototype iteration. The footprint of the tool could potentially also be optimized to reduce the overall volume that the tool occupies when installed in a lab. The resolution and positional accuracy of the motion platform should also be confirmed with empirical testing. Ideally, testing would be completed to determine if the minimal incremental motion (MIM) of the tool matches the calculated value of 5 μm . If the MIM value were verified, optical scale encoders could be mounted to the tool – especially since mounting points have already been included in the design and are machined in the current prototype. The inclusion of encoders could enable a positioning feedback system to be integrated into the tool’s software to ensure the optical probe head is in its intended location. Note that this modification is only necessary if imaging capabilities are desired from the tool. In the current prototype, the resolution and accuracy requirements specified in Table 5-1 are much more precise than required since the characterization tests of interest are specifically focused on bulk device performance. More specifically, the current testing capabilities assume that the data of interests can be collected at a single point (or relatively few points) on a sample and confidently represent the overall performance characteristics of the solar cell. If bulk performance continues to be the target of future measurements with the tool, it may even be beneficial to replace the current lead screw assemblies with a larger lead alternative to increase the speed in which the probe head can travel.

Finally, future efforts must verify the accuracy of the data the tool is capable of collecting. Batches of stable samples should be measured with both existing standardized characterization techniques and with the tool prototype. This testing would ensure that the data the tool is collecting

not only matches the quality of data collected with existing measurement tools, but also provides additional value in speed, ease of use, and novel physical insights.

7. Conclusions

The optical characterization tool prototype validates the potential to improve upon existing measurement tools and increase the pace of PV research. Most notably, the tool has achieved successful measurement of PL and TRPL, autonomous data collection, and rapid adaptability to various optical configurations for different measurement techniques. Moving forward, this prototype can be further refined and modified to better suit the needs of research applications the GridEdge Solar team is most interested in pursuing. More specifically, changes to the lead screws will enable much faster tool motion while providing adequate positioning capabilities for measuring bulk performance characteristics of PV devices. Alternatively, efforts could focus on enabling imaging capabilities and ensuring the tools motion platform operates at an exacting resolution via the incorporation of linear scale encoders and an active positioning control system. In either case, the current prototype provides a useful foundation for future work and could serve as a meaningful milestone in the pursuit of commercial-ready high-throughput characterization tool.

8. References

- [1] “SunShot 2030 White Paper.Pdf.”
- [2] “Electric Power Annual 2019,” p. 240.
- [3] “Perovskite Solar Cells,” Energy.gov [Online]. Available: <https://www.energy.gov/eere/solar/perovskite-solar-cells>. [Accessed: 29-Apr-2021].
- [4] Kirchartz, T., Márquez, J. A., Stolterfoht, M., and Unold, T., 2020, “Photoluminescence-Based Characterization of Halide Perovskites for Photovoltaics,” *Advanced Energy Materials*, **10**(26), p. 1904134.
- [5] de Quilettes, D. W., Vorpahl, S. M., Stranks, S. D., Nagaoka, H., Eperon, G. E., Ziffer, M. E., Snaith, H. J., and Ginger, D. S., 2015, “Impact of Microstructure on Local Carrier Lifetime in Perovskite Solar Cells,” *Science*, **348**(6235), pp. 683–686.
- [6] Paschotta, D. R., “Lambertian Emitters and Scatterers” [Online]. Available: https://www.rp-photonics.com/lambertian_emitters_and_scatterers.html. [Accessed: 01-May-2021].
- [7] “Ergonomics ETool: Solutions for Electrical Contractors - Materials Handling: Heavy Lifting” [Online]. Available: <https://www.osha.gov/SLTC/etools/electricalcontractors/materials/heavy.html>. [Accessed: 01-May-2021].
- [8] “Product-Catalog-Lead-Screw-Technology.Pdf.”